CHEMBIOCHEM

DOI: 10.1002/cbic.200800345

Efficient DNA Binding and Nuclear Uptake by Distamycin Derivatives Conjugated to Octa-arginine Sequences

Olalla Vázquez,[a] Juan B. Blanco-Canosa,[a] M. Eugenio Vázquez,[a] Jose Martínez-Costas,[b] Luis Castedo,[a] and José L. Mascareñas*[a]

Efficient targeting of DNA by designed molecules requires not only careful fine-tuning of their DNA-recognition properties, but also appropriate cell internalization of the compounds so that they can reach the cell nucleus in a short period of time. Previous observations in our group on the relatively high affinity displayed by conjugates between distamycin derivatives and bZIP basic regions for A-rich DNA sites, led us to investigate whether the covalent attachment of a positively charged cell-penetrating peptide to a distamycin-like tripyrrole might yield high affinity DNA binders with improved cell internalization properties. Our work has led to the discovery of synthetic tripyrrole–octa-arginine conjugates that are capable of targeting specific DNA sites that contain A-rich tracts with low nanomolar affinity; they simultaneously exhibit excellent membrane and nuclear translocation properties in living HeLa cells.

Introduction

Recent decades have witnessed the development of a variety of strategies to achieve high-affinity, sequence-specific DNA recognition with unnatural synthetic agents.[1] These molecules interact with DNA either through the major groove, as in the case of triplex-forming oligonucleotides,[2] customized zinc finger proteins[3] or minimized versions of transcription factors,[4] or by contacting the DNA minor groove, as with pyrrole/imidazole polyamides.[5] Our group has also developed a DNA-recognition strategy based on simultaneous, bipartite binding in both the major and minor grooves.[6] A major obstacle in developing these agents as practical, specific gene-modulating reagents derives from their intrinsic difficulty in crossing the cell membrane and entering the nucleus. Recent studies with DNA-binding polyamides suggest that their cellular and nuclear uptake is a rather slow process and is quite dependent on the structural characteristics of the molecule.[7]

In our initial studies aimed at the development of bivalent major/minor groove DNA binders based on hybrids between distamycin-related tripyrroles and the basic region of the bZIP protein GCN4, we observed unexpectedly high-affinity interactions with double-stranded (ds) DNA molecules that contained A-rich tracts but lacked the consensus binding site for the bZIP basic region.[6c–e] This result was explained in terms of the highly basic peptide that complemented the specific interaction of the tripyrrole moiety in the A-rich minor groove, by establishing unspecific, salt bridges with the negatively charged DNA phosphate backbone.[8]

On the basis of these observations and the well-established cell transport properties of highly charged basic regions that contain polyarginine tracts,[9] we reasoned that tethering a DNA minor-groove binding moiety to appropriate oligo-arginine fragments could lead to high affinity DNA binders with improved cell uptake properties (Figure 1). Herein, we report the synthesis, DNA binding and HeLa cell internalization studies of conjugates between distamycin tripyrrole analogues and several peptide sequences. These studies led to the discovery of a hybrid equipped with an octa-arginine peptide that in addition to exhibiting excellent nuclear localization properties binds specifically to A-rich DNA sites with significantly high affinity.

Results and Discussion

Design and synthesis of conjugates

Well-established structural data on the interaction of distamycin analogues with the minor groove of A-rich DNA sequences,[10] suggest that the pyrrole nitrogens are the best positions for attaching the required oligo-arginine peptides, since modifications on these atoms should not disturb the DNA-contacting surface of the tripyrrole molecule. Direct fluorescent analysis of the cell transport properties of the resulting hybrids is precluded by the extremely low fluorescence quantum yield of distamycin,[11] and, therefore, we decided to incorporate an extrinsic fluorophore (fluorescein) into the conjugates. On this basis, and taking into account synthesis considerations, we de-

[a] *O. Vázquez, Dr. J. B. Blanco-Canosa, Dr. M. E. Vázquez, Dr. L. Castedo, Dr. J. L. Mascareñas*
Departamento de Química Orgánica
Universidad de Santiago de Compostela
15782 Santiago de Compostela (Spain)
Fax: (+34) 981-59-59-12
E-mail: joseluis.mascarenas@usc.es

[b] *Dr. J. Martínez-Costas*
Departamento de Bioquímica y Biología Molecular
Universidad de Santiago de Compostela
15782 Santiago de Compostela (Spain)

Supporting information for this article is available on the WWW under http://www.chembiochem.org or from the author.

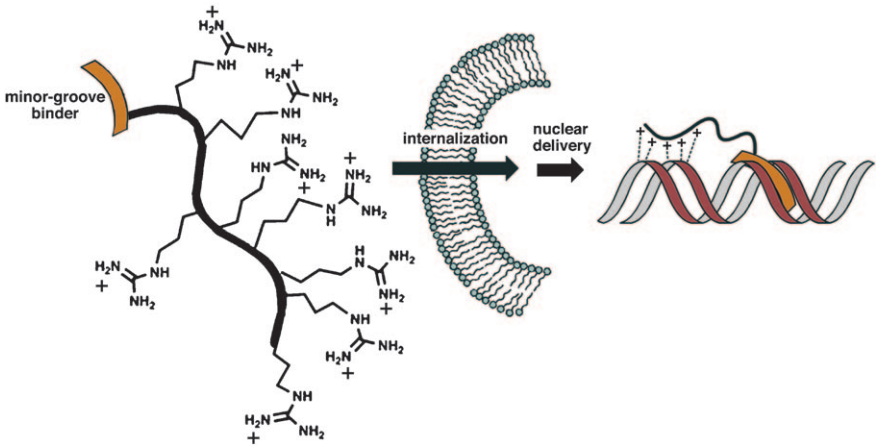

Figure 1. Schematic outline of our hypothesis.

cided to target the tripyrrole–peptide conjugate **1A**, in which the tripyrrole is orthogonally linked to the side chain of a lysine amino acid incorporated at the N terminus of the peptide sequence through an aminohexanoic acid spacer (Scheme 1). This hybrid could be assembled by means of a convergent strategy that involved the independent elaboration of the lysine-containing peptide and an appropriate aminotripyrrole **6**.[6e,f]

The versatility of this approach should allow the preparation of other derivatives with different peptide sequences, such as conjugate **2A**, which features a less basic peptide (IAAKRGQLD) that has been shown to serve as a nuclear localization signal (NLS).[12] In addition to probing nuclear and plasma membrane properties, this hybrid might be invaluable as a control to validate the effect of the octa-arginine moiety on the DNA-binding properties of the synthetic constructs. Assuming that the presence of the oligo-arginine unit might not be enough to ensure the correct delivery of the peptides to the cell nuclei, we also pursued the preparation of compounds that incorporated both peptidic sequences, NLS and octa-arginine, either coupled in a linear arrangement through the peptidic backbone (conjugate **4A**) or by means of a reductively labile disulfide bond (disulfide **5A**).

As additional controls we also prepared the mutant derivative **3A**, which features an Arg to Ala mutation in the NLS sequence and has previously been reported to completely suppress the ability of this peptide to mediate nuclear transport,[13] and the fluorescein-tripyrrole derivative **7** (Scheme 2). To evaluate the functional relevance and influence of the tripyrrole unit we also prepared the fluorescein–peptide hybrids **1B**–**4B** (Scheme 1), which consist exclusively of the peptidic counterparts of the above conjugates.

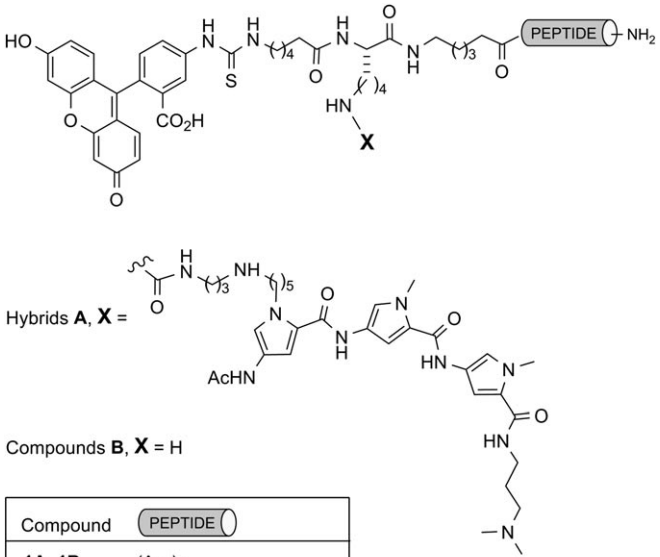

Compound	PEPTIDE
1A, **1B**	$(Arg)_8$
2A, **2B**	IAAKRGRQLD
3A, **3B**	IAAKRGAQLD
4A, **4B**	IAAKRGRQLD-G -$(Arg)_8$
5A	C-IAAKRGRQLD S-S Aba-C -$(Arg)_8$-NH_2

Scheme 1. Designed tripyrrole–peptide conjugates, Aba = *p*-acetamidobenzoyl.

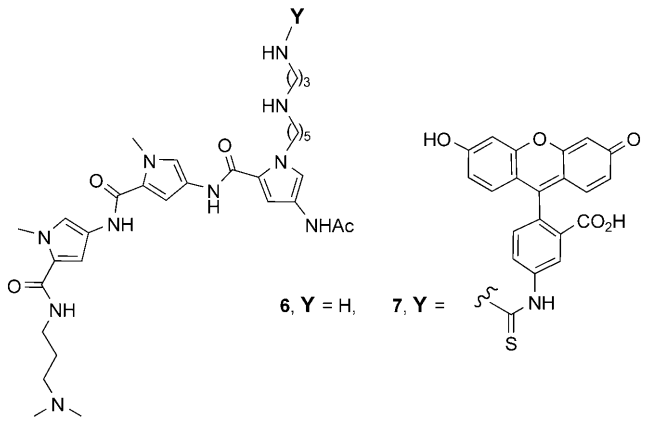

Scheme 2. Fluorescein–tripyrrole derivatives **6** and **7**.

Synthesis of the peptidic fragments was carried out by using standard Fmoc solid-phase methods. The lysine required to attach the minor-groove binding moiety to the peptide was introduced with an Alloc-protected side chain. Attachment of fluorescein to the amino terminus was performed by coupling of the free N-terminal amine peptide with fluorescein isothiocyanate. Removal of the Alloc-protecting group followed by standard peptidic cleavage–deprotection and purification led to the tripyrrole-lacking peptides **1B**–**4B** (Scheme 3, steps a–e and h). Attachment of the minor-groove binding tripyrrole to

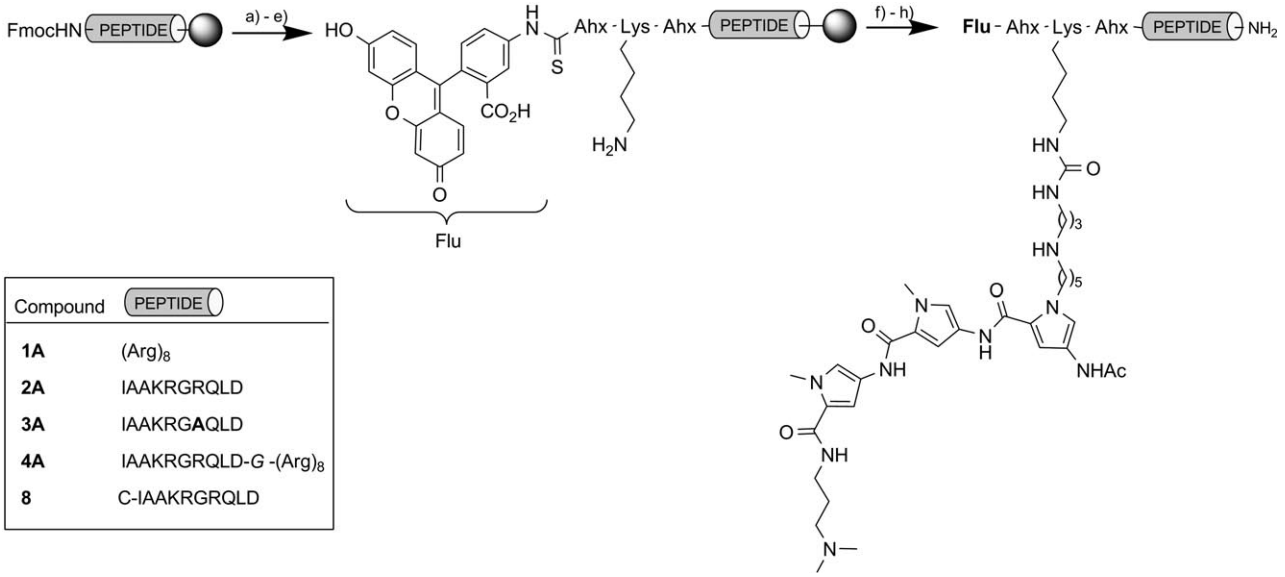

Compound	PEPTIDE
1A	$(Arg)_8$
2A	IAAKRGRQLD
3A	IAAKRG**A**QLD
4A	IAAKRGRQLD-*G*-$(Arg)_8$
8	C-IAAKRGRQLD

Scheme 3. General scheme for the synthesis of hybrids **1A**–**4A**: a) i. 20% piperidine in DMF; ii. HOBT/HBTU, DIEA/DMF, Fmoc-Ahx-OH; b) i. 20% piperidine in DMF; ii. HOBT/HBTU, DIEA/DMF, Fmoc-Lys(Alloc)-OH; c) i. 20% piperidine in DMF; ii. HOBT/HBTU, DIEA/DMF, Fmoc-Ahx-OH; d) 0.5 M DIEA in DMF, FITC (fluorescein isothiocyanate, 4 equiv); e) $[Pd(PPh_3)_4]$ (1 equiv), morpholine (190 equiv), 2% H_2O/CH_2Cl_2, 5 h; f) 0.5 M DIEA in DMF, DMAP/DMF, *N*,*N*′-disuccinimidyl carbonate; g) 0.5 M DIEA in DMF, DMF and the aminotripyrrole **6**; h) 90% TFA, 50% CH_2Cl_2, 2.5% H_2O and 2.5% TIS, room temperature. Ahx: 6-aminohexanoic acid; DIEA: *N*,*N*-diisopropylethylamine; TIS: triisopropylsilane; FITC: fluorescein isothiocyanate.

the peptides was performed when these were still bound to the solid support and fully protected, except at the lysine side chain. The coupling reaction was carried out by sequential addition of the bifunctional conjugating agent disuccinimidyl carbonate and the aminotripyrrole **6**. After the standard cleavage–deprotection and purification steps, we efficiently obtained hybrids **1A**–**4A** as well as the cysteine-containing derivative **8**. Disulfide derivative **5A** was prepared by convergent coupling between **8** and an activated cysteine–octa-arginine peptide (see the Supporting Information). On the other hand, fluorescein-labelled tripyrrole derivative **7** was efficiently prepared by coupling fluorescein isothiocyanate to aminopyrrole **6** (Supporting Information).

Cell-internalization studies

Cellular uptake of the synthetic constructs was studied in HeLa cells, and analyzed after fixation of the cells by registering fluorescence images at three different time points: 30 min, 90 min and 3 h after incubation with the compounds. The results obtained at each time point were qualitatively similar, although the dataset obtained after 90 min incubation was considered to be the most representative since sampling after 30 min generally showed an incomplete distribution of the molecules inside the cells, and the data obtained after 3 h incubation exhibited saturated fluorescence emission that prevented a clear interpretation of the images. Analysis of the cells before fixation gave similar results; this confirmed that the fixation conditions did not generate artificial redistribution of the molecules, which could lead to false-positives or undesirable artefacts in the samples. Moreover, this treatment not only facilitated the recording of the images, but also allowed long-term storage of the specimens.

As shown in Figure 2A, incubation of cells with 2 μM octa-arginine–tripyrrole conjugate **1A** for 90 min at 37 °C led to the appearance of a very intense and homogeneous fluorescence signal that was concentrated in the cell nuclei. Therefore, it seems that the octa-arginine not only helps the tripyrrole to cross the cytoplasmatic membrane, but it also provides for nuclear localization, at least when conjugated to the tripyrrole. Strong fluorescence was observed in the nuclei even after only 30 min incubation (Supporting Information); this suggests a very rapid uptake of **1A**. This is particularly relevant since DNA-binding polyamides that lack appended peptides require much longer incubation periods to reach the cell nucleus.[7]

In the case of hybrid **2A**, which incorporates a nuclear localization signal (NLS: IAAKRGRQLD) instead of the octa-arginine, we observed low intracellular fluorescence that was mainly located in the nuclei (Figure 2B). The lower fluorescence intensity compared with hybrid **1A** is probably because the NLS sequence of **2A** promotes a less efficient cytoplasmic uptake than the Arg_8 sequence present in **1A**. Attachment of the octa-arginine sequence to the NLS hybrid, either through a linear arrangement (**4A**) or by means of a reductively labile disulfide bond (**5A**), restored an efficient cell-membrane crossing ability. Hence, incubation of the cells with conjugates **4A** and **5A** led to a more intense fluorescence in the nucleus than in the case of compound **2A** (Figures 2C and D). It should be noted, however, that the observed fluorescence intensity promoted by **4A** and **5A** was not as strong as with **1A**. The fluorescence intensity observed with compound **4A** was somewhat higher than that obtained for **5A** (note that Figures 2C and D were acquired with different exposure times), perhaps

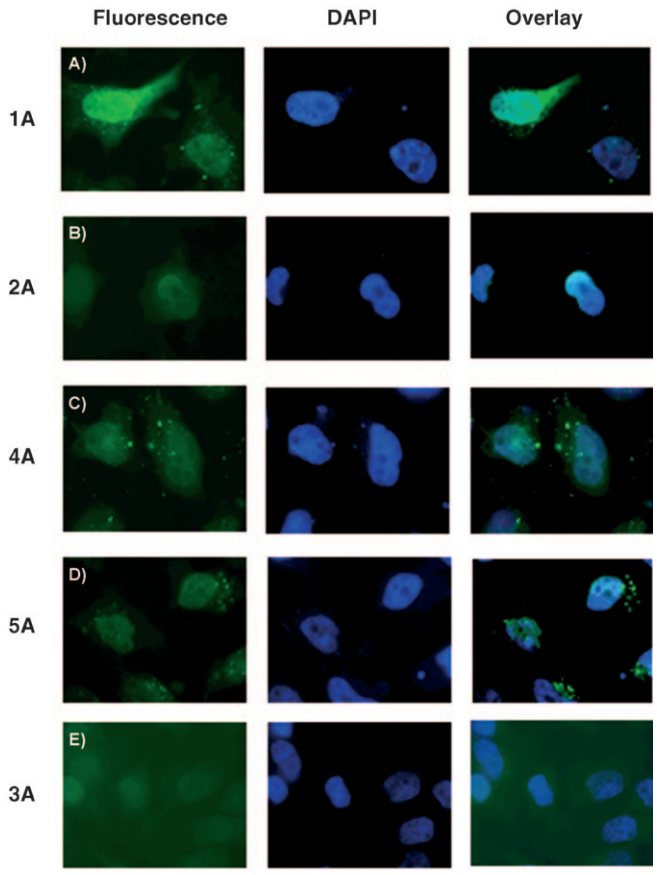

Figure 2. Intracellular distribution in HeLa cells. Exposure times were set for each sample due to the variations in overall emission intensity resulting from the different uptake efficiencies. Exposure times: **1A**, **4A** = 1/18 s; **2A** = 1/2 s; **5A** = 1/6 s; **3A** = 1 s; DAPI (4′,6-diamidino-2-phenylindole) is a well known nuclear stain.

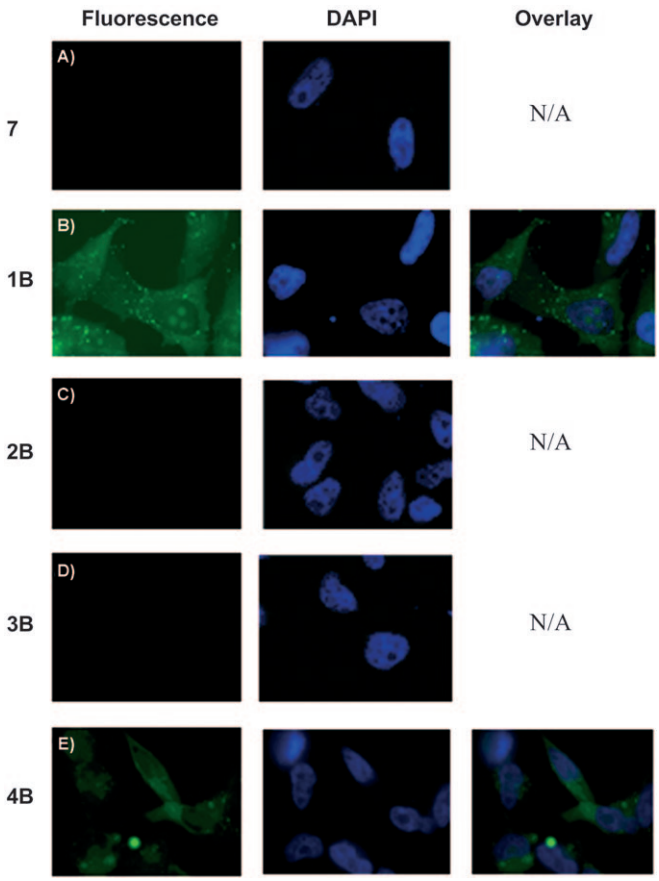

Figure 3. Intracellular distribution in HeLa cells. Exposure times were: **1B** = 1/18 s; **7**, **2B**, **3B**, **4B** = 1/6 s.

as a consequence of partial cleavage of the disulfide bond after entering the cell.[14] Conjugate **3A**, which features a mutation in the NLS sequence in comparison to **2A**, promoted a weak and diffuse fluorescence that was evenly distributed between the nucleus and the cytoplasm (Figure 2E).

Tripyrrole **7**, which lacks the cell-penetrating peptide sequence, was unable to induce intracellular cell fluorescence even after 3 h incubation (Figure 3A). This result supports the critical role of the octa-arginine peptide unit for efficient cell translocation. On the other hand, removal of the DNA-binding tripyrrole had a significant influence on the intracellular localization of the molecules. Therefore, octa-arginine **1B** leads to an intense cellular fluorescence but, in contrast to conjugate **1A**, it is predominantly located in the cytoplasm (Figure 3B). Peptides **2B** and **3B**, which lack the oligo-arginine fragment, were not able to enter the cells, as evidenced by the fact that intracellular fluorescence could not be detected.

Peptide **4B**, which contains the arginine oligomer and the NLS sequence, displayed intracellular cytoplasmatic localization, although the fluorescence signal was weak and faded. As in the case of the tripyrrole-containing analogues, the presence of the NLS complement in the octa-arginine peptides did not provide any beneficial effect on the cellular uptake properties of the compounds: **1B** led to higher intracellular fluorescence than **4B**. Taken together, these results are consistent with an efficient cellular entry of the conjugates that bear the octa-arginine sequence; in particular **1A** rapidly and efficiently accumulated inside the cell nuclei, probably because of thermodynamic trapping of the hybrid on the chromosomes. In the absence of the minor-groove binding unit, the octa-arginine-bearing compounds populate the cytoplasm but not the nucleus. Therefore, nuclear delivery was facilitated by the concomitant presence of both the oligo-arginine moiety and the minor groove DNA-binding unit.

DNA-binding assays

Once the cell transport advantages resulting from the attachment of an oligo-arginine to the DNA minor-groove binder was demonstrated, we wanted to see whether the presence of the highly charged peptide contributes to an increase in the DNA-binding affinity of the hybrid molecule.

Although the DNA interaction of a synthetic minor-groove binder cannot usually be analyzed with standard electrophoretic mobility shift assays (EMSAs), we assumed that the presence of the conjugated octapeptide might allow the observation of gel shifts in this type of experiment. Accordingly, addition of increasing concentrations of hybrid **1A** to a ^{32}P-labelled

double stranded oligonucleotide containing the target sequence (ATTTT) promoted the appearance of slower migrating bands, which must correspond to peptide–DNA complexes (Figure 4A). As expected, the interaction requires the presence of the TTTT tract since incubation with double stranded oligonucleotides lacking such sequences did not induce the formation of complexation bands in the gel shift experiments (Figure 4B). Octa-arginine **1B** was unable to generate any gel shift even at peptide concentrations of 500 nM (Figure 4C); this is consistent with the requirement of the tripyrrole for the DNA interaction.

As observed in the gels presented in Figure 4A, the shifted bands were quite diffuse and even disappeared in the presence of high peptide concentrations. Considering that these anomalous results might derive from the presence of the planar, hydrophobic fluorescein, which could adversely affect the solubility and gel migration properties of the DNA–conjugate complexes,[15] we decided to run the gel shift titration experiment with conjugate **9**, which is analogous to **1A** but lacks the fluorophore unit (synthesis described in the Supporting Information).

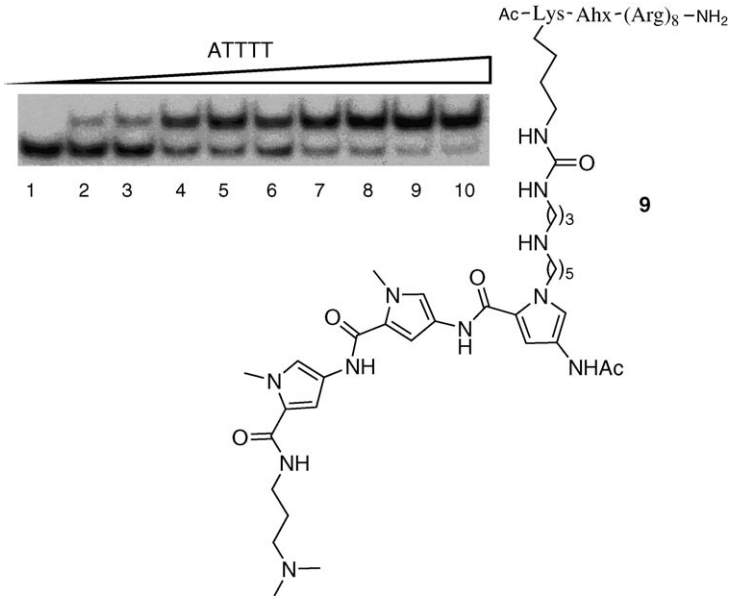

Figure 5. EMSA results showing the binding of peptide **9** to dsDNA ATTTT. The experiment was carried out with 45 pM DNA. Lanes 1–10 [**9**] = 0, 2, 4, 6, 8, 10, 12, 15, 20, 25 nM; Ahx = 6-aminohexanoic.

It was gratifying to find that conjugate **9** gave a well-defined gel shift result, which corresponds with a high affinity dsDNA interaction (Figure 5). Titration at room temperature enabled the calculation of a dissociation constant of (6 ± 0.5) nM, for a 1:1 binding mode, which is approximately two orders of magnitude higher than that of distamycin.[10] This confirms that the presence of the arginine tether effectively increased the DNA-binding affinity of the minor-groove binder. The relevance of the oligo-arginine for DNA interaction was further demonstrated by observing that a hybrid analogue of **2A** that lacked the fluorescein unit (**10**) interacted with the dsDNA ATTTT with much lower affinity than **9** (Figure 6A). Attachment of the oligo-arginine moiety to the minor-groove binder did not compromise the sequence selectivity as evidenced by comparative gel shift experiments that demonstrated the requirement of at least a TTTT sequence for the detection of high affinity interactions (Figure 6B).

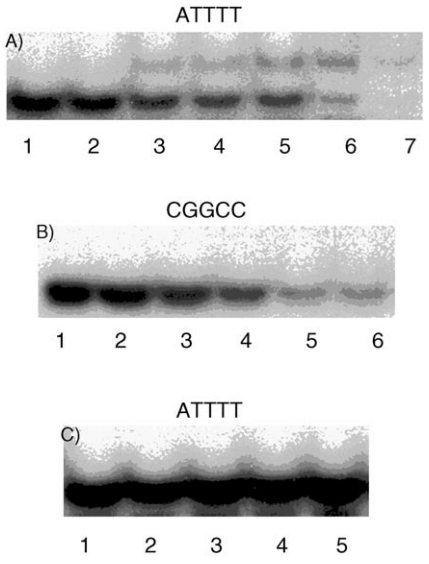

Figure 4. EMSA results showing the binding of conjugates: A) and B) **1A**, and C) **1B** to different dsDNA molecules. Experiments were carried out with 45 pM ^{32}P–dsDNA and increasing concentrations of the conjugates at room temperature. Binding experiments were carried out in Tris·HCl (18 mM; pH 7.5), KCl (90 mM), $MgCl_2$ (1.8 mM), EDTA (1.8 mM), glycerol (9%), BSA (0.11 mg mL^{-1}) and NP-40 (4.4%). A) Conjugate **1A** in the presence of dsDNA ATTTT (5′-GAGG*ATTTT*CAGCTTACGCT-3′), lanes 1–7 [**1A**] = 0, 5, 20, 50, 100, 150, 200 nM; B) conjugate **1A** in the presence of dsDNA CGGCC (5′-GAGG*CGGCC*ATGACGTTCGT-3′); lanes 1–6 [**1A**] = 0, 50, 100, 200, 300, 500 nM; C) conjugate **1B** in the presence of dsDNA ATTTT; lanes 1–5 [**1B**] = 0, 50, 150, 250, 500 nM.

Conclusions

Distamycin-like minor-groove DNA binders reach the cell nucleus with difficulty due to their poor membrane permeability. We have demonstrated that appropriate linkage of these molecules to octa-arginine fragments not only allows rapid localization in the cell nuclei but also induces a very remarkable (over 100-fold) increase in affinity for A-rich dsDNA sites. Moreover, we have observed significant synergistic transport effects between the minor-groove binding tripyrrole unit and the octa-arginine peptide, which cooperate in localizing the hybrid molecules in the cell nuclei. Our studies further show that the inclusion of an additional NLS sequence in the structure of the conjugates does not provide any significant transport benefits and can even be counterproductive. The strategy presented here should also work for other minor-groove binders and might allow the efficient delivery of desired cargoes to the chromosome.

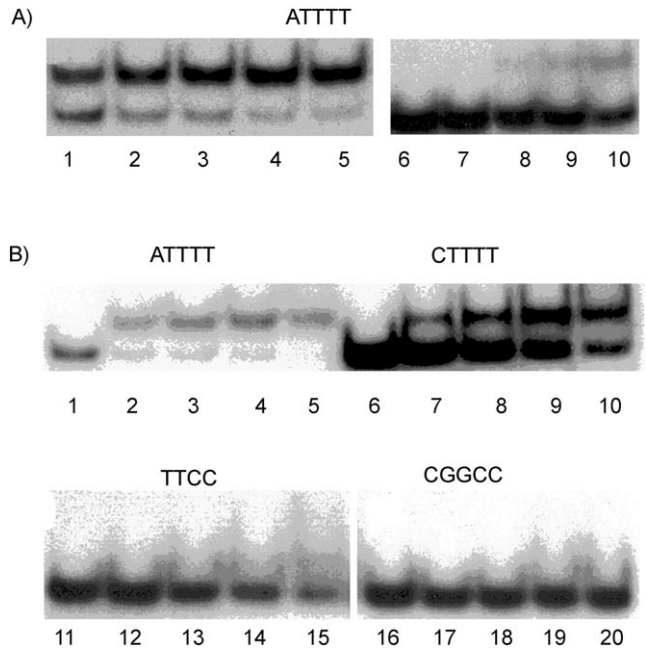

Figure 6. EMSA results showing the binding of peptides **9** and **10** to dsDNA molecules. The experiments were carried out with 45 pM of DNA. A) Lanes 1–6: dsDNA ATTTT + [**9**] = 10, 12, 15, 20, 25 nM; lanes 6–10: dsDNA ATTTT + [**10**] = 50, 100, 200, 300, 500 nM; B) dsDNAs + [**9**] = 0, 20, 50, 100, 150 nM; lanes 1–5: dsDNA ATTTT; lanes 6–10: dsDNA CTTTT; lanes 11–15: dsDNA TTCC; lanes 16–20: dsDNA CGGCC; dsDNA CTTTT: 5′-GAGGC*CTTTT*GAGAG-TGCCT-3′; dsDNA TTCC: 5′-GAGGC*TTCC*ATGACGTTCGT-3′.

Experimental Section

General: Solvents and reagents were purchased from commercial sources and were used without further purification (see the Supporting Information). Fmoc-protected amino acids were featured with standard side-chain protecting groups [Fmoc-Ala-OH, Fmoc-Arg(Pbf)-OH, Fmoc-Cys(Trt)-OH, Fmoc-Asp(*t*Bu)-OH, Fmoc-Gln(Trt)-OH, Fmoc-Gly-OH, Fmoc-Leu-OH, Fmoc-Lys(Boc)-OH and Fmoc-Ile-OH], except for the lysine residue required for orthogonal ligation [Fmoc-Lys(Alloc)-OH]. Water was purified by using a Millipore MilliQ water purification system.

High-performance liquid chromatography: HPLC was performed by using an Agilent 1100 series liquid chromatograph mass spectrometer system equipped with a MWD (multiple wavelength detector). Analytical HPLC was carried out by using a C_{18} LiChrospher WP 300 RP-18 (5 μm) analytical column. Purification of the peptides was performed by using a Nucleosil 120–10 RP-18 (250×8) column. Standard conditions for analytical and preparative HPLC consisted of an isocratic regime during the first 5 min, followed by a linear gradient from 5 to 75% of solvent B for 30 min (A: water with 0.1% TFA, B: acetonitrile with 0.1% TFA). Compounds were detected by UV absorption at 220, 270 and/or 304 nm.

Mass spectrometry: Electrospray ionization mass spectrometry was performed by using an Agilent 1100 series LC/MSD model in positive scan mode with direct injection of the purified peptide solution into the instrument.

Peptide synthesis and purification: Peptides were synthesized manually on the 0.1 mmol scale by following standard Fmoc solid-phase methods and by using a Fmoc-PAL-PEG-PS (0.19 mmol g^{-1}) resin. Each amino acid was activated for 2 min in DMF prior to addition onto the resin. Peptide bond-forming couplings were conducted for 45 min to 1 h and monitored by using the trinitrobenzenesulfonic acid (TNBS) test.[16] Deprotection of the temporal Fmoc protecting group was performed by treating the resin with piperidine (20%) in DMF for 15 min. The final peptides were obtained after the cleavage-deprotection step, which was carried out by using a standard TFA cleavage cocktail as outlined below.

Deprotection of the temporal Fmoc group: Piperidine (5 mL, 20% in DMF) was added to 0.1 mmol of resin-linked Fmoc-peptide and nitrogen was passed through the mixture for 15 min. The resin was then filtered off and washed with DMF (3×5 mL×3 min). The complete removal of Fmoc was monitored by running a TNBS test with a small resin sample.

Coupling of amino acids: DIEA (3 mL of 0.195 M solution in DMF) was added to a solution of the Fmoc-amino acid (0.4 mmol) dissolved in a solution of HOBt/HBTU in DMF (2 mL of 0.2 M HBTU, 0.2 M HOBt). The resulting mixture was stirred for 2 min and then added over the resin. Nitrogen was passed through the resin suspension for 45 min until the coupling was complete according to the TNBS test on a small resin aliquot. The resin was filtered off and washed with DMF (3×5 mL×3 min). Peptide synthesis was continued with the next deprotection–coupling cycles in a similar fashion.

Selective deprotection of the Lys(Alloc) side chain:[17] Once the peptide sequence was completed, selective deprotection of the lysine residue was carried out by using the following procedure: peptide (0.1 mmol) attached to the solid support was treated at room temperature for 5 h with a mixture of $Pd(PPh_3)_4$ (1 equiv) and morpholine (190 equiv) in 2% H_2O/CH_2Cl_2 (5 mL). The resin was filtered off and washed with DMF (2×5 mL×2 min), diethyldithiocarbamate (DEDTC, 25 mg in 5 mL of DMF, 2×5 min), DMF (2×5 mL×2 min) and CH_2Cl_2 (2×5 mL×2 min).

Cleavage–deprotection step: The resin-bound peptide was dried and treated with the cleavage cocktail (50 μL of CH_2Cl_2, 25 μL of water, 25 μL of TIS, and TFA up to 1 mL for 40 mg of resin). For peptides incorporating ethane-1,2-dithiol cysteine residues, the following cleavage cocktail was used: EDT (25 μL), H_2O (25 μL), TIS (10 μL) and TFA up to 1 mL for 40 mg of resin. The resulting suspension was shaken for 2 h, the resin was filtered off and the TFA filtrate was added to ice-cold Et_2O (10 mL of Et_2O for each mL of TFA). After 10 min, the mixture was centrifuged and the solid was washed with ice-cold Et_2O (20 mL). The solid residue was dried under argon, dissolved in acetonitrile/water (1:1, 2 mL), purified by preparative reverse-phase HPLC, and identified by mass spectrometry. The collected fractions were lyophilized and stored at −20 °C.

Synthesis of fluorescent hybrids: The N-terminal Fmoc-protected residue of the peptidyl resin was removed by following the standard procedure. The resin was washed and a solution of DIEA (0.5 M, 6 equiv) in DMF and fluorescein isothiocyanate (FITC, 4 equiv) were added. The resulting mixture was stirred for 1 h at room temperature. The resin was washed with DMF (2×5 mL) and the Alloc-protecting group was selectively removed as explained above. The resulting peptidyl resin was either subjected to the cleavage–deprotection and purification step to make derivatives **1B**–**4B** or coupled with the aminotripyrrole unit to make derivatives **1A**–**4A**. For such a coupling the resin was resuspended in DMF (1 mL) and shaken for 30 min to ensure good swelling. The DMF was removed from the resin by filtration and DIEA (0.5 M) in DMF (8 equiv), DMAP in DMF (2 equiv) and *N,N*′-disuccinimidyl carbonate (15 equiv) were added. The resulting mixture was shaken for 2 h. The resin was washed with DMF and a solution of aminotripyrrole **6**[6e,f] in DMF (4 equiv), DIEA (0.5 M) in DMF (8 equiv) and

DMAP (2 equiv) were added. The reaction mixture was shaken for 2 h and the resin was washed with DMF (2×5 mL×2 min), Et_2O and dried. Cleavage–deprotection under standard conditions afforded the expected conjugates, which were purified by reversed-phase HPLC and identified by mass spectrometry.

Synthesis of S–S hybrid 5A: This compound was obtained by coupling the corresponding cysteine-containing peptide with the cysteine–octa-arginine peptide previously activated by treatment with DTNB (Ellman's reagent).[18] The coupling reaction was performed in a buffered solution consisting of Tris·HCl (100 mM, pH 7.5) and NaCl (1 M) and the mixture was stirred for 45 min at room temperature. The disulfide product was purified by RP-HPLC and identified by mass spectrometry.

UV spectroscopy: The peptides, conjugates and DNA concentrations of the solutions used in the experiments were determined by UV spectroscopy. UV measurements were carried out in a SmartSpec Plus spectrophotometer by using standard semimicrovolume disposable polystyrene cuvettes. Concentrations were measured by using known extinction coefficients of the chromophores (Supporting Information).

Gel mobility shift assays: Binding reactions were performed for 30 min at room temperature in a mixture (20 μL) containing Tris·HCl (18 mM, pH 7.5), KCl (90 mM), $MgCl_2$ (1.8 mM), EDTA (1.8 mM), glycerol (9%), BSA (0.11 mg mL^{-1}) and NP-40 (4.4%). The experiments with ^{32}P-labelled DNA molecules were carried out by using labelled dsDNA (approximately 45 pM). Products were resolved by PAGE by using a nondenaturing polyacrylamide gel (15%) and 0.5×TBE buffer (44.5 mM Tris, 44.5 mM boric acid, 1 mM EDTA, pH 8.0) and analyzed by autoradiography.

Cell uptake experiments and fluorescence analysis: HeLa cells were maintained in DMEM (Dulbecco Modified Eagle Medium) containing FBS (foetal bovine serum; 10%). The day before the cellular uptake experiments, cells were seeded in 12-well plates containing glass coverslips (15 mm). Cells were then washed three times in PBS and overlayed with fresh DMEM (1 mL; without serum). The different compounds tested were then added in order to obtain a final concentration of 2 μM and the samples were incubated at 37 °C. After incubation, cells were washed three times with PBS to remove excess compound and they were analysed either before or after fixation by using a fluorescence microscope. Samples were analyzed 30, 90 and 180 min after the addition of the compounds. The fixation was carried out by treatment with paraformaldehyde (4%) in PBS containing DAPI (to stain the nuclei; 300 nM) at 4 °C for 15 min. After fixation, the coverslips were washed three times with PBS and mounted on glass slides with Mowiol 4-88® (100 mg mL^{-1} in 100 mM Tris·HCl, pH 8.5, 25% glycerol, 0.1% DABCO as an antifading agent) prior to observation by fluorescence microscopy. Images were obtained with an Olympus DP-50 digital camera mounted on an Olympus BX51 fluorescence microscope and were further processed (cropping, resizing and contrast and brightness adjustment) with Adobe Photoshop (Adobe Systems).

Acknowledgements

This work was supported by the Spanish grants SAF2007–61015, CTQ2006–01339, SAF2006–06868 and Consolider Ingenio 2010 (CSD2007–00006), the Xunta de Galicia (PGIDIT06PXIB209018PR and GRC2006/132) and the Human Frontier Science Program (CDA0032/2005-C). O.V. and J.B.B. thank the Spanish MEC for their Ph.D. fellowships, and M.E.V. thanks the Spanish MEC for his Ramon y Cajal contract.

Keywords: cell transport · distamycin · DNA recognition · DNA · octa-arginine

[1] a) S. Neidle, *Nucleic Acid Structure and Recognition*, Oxford University Press, **2002**; b) L. Strekowski, B. Wilson, *Mutat. Res., Fundam. Mol. Mech. Mutagen.* **2007**, *623*, 3–13; c) B. S. P. Reddy, S. M. Sondhi, J. W. Lown, *Pharmacol. Ther.* **1999**, *84*, 1–111.

[2] a) C. Escude, *Top. Curr. Chem.* **2005**, *253*, 109–148; b) S. O. Doronina, J. P. Behr, *Chem. Soc. Rev.* **1997**, *26*, 63–71.

[3] a) M. Dhanasekaran, S. Negi, Y. Sugiura, *Acc. Chem. Res.* **2006**, *39*, 45–52; b) S. A. Wolfe, L. Nekludova, C. O. Pabo, *Annu. Rev. Biophys. Biomol. Struct.* **2000**, *29*, 183–212; c) C. O. Pabo, *Annu. Rev. Biochem.* **2001**, *70*, 313–340.

[4] a) M. E. Vázquez, L. Castedo, J. L. Mascareñas, *Chem. Soc. Rev.* **2003**, *32*, 338–349; b) D. K. Lee, W. Seol, J. S. Kim, *Curr. Top. Med. Chem.* **2003**, *3*, 645–657; c) S. Sato, M. Hagihara, K. Sugimoto, T. Morii, *Chem. Eur. J.* **2002**, *8*, 5066–5071; d) A. Z. Ansari, A. K. Mapp, *Curr. Opin. Chem. Biol.* **2002**, *6*, 765–772.

[5] a) P. B. Dervan, A. T. Poulin-Kerstien, E. J. Fechter, B. S. Edelson, *Top. Current Chem.* **2005**, *253*, 1–31; b) P. B. Dervan, R. M. Doss, M. A. Marques, *Curr. Med. Chem. Anti-Cancer Agents* **2005**, *5*, 373–387; for general reviews on DNA minor-groove recognition, see: c) S. M. Nelson, L. R. Ferguson, W. A. Denny, *Mutat. Res., Fundam. Mol. Mech. Mutagen.* **2007**, *623*, 24–40; d) U. Pindur, M. Jansen, T. Lemster, *Curr. Med. Chem.* **2005**, *12*, 2805–2847; e) W. C. Tse, D. L. Boger, *Chem. Biol.* **2004**, *11*, 1607–1617; f) S. Neidle, *Nat. Prod. Rep.* **2001**, *18*, 291–309; g) D. E. Wemmer, *Annu. Rev. Biophys. Biomol. Struct.* **2000**, *29*, 439–461; h) V. I. Dodero, M. Mosquera, J. B. Blanco, L. Castedo, J. L. Mascareñas, *Org. Lett.* **2006**, *8*, 4433–4436, and references therein.

[6] a) O. Vázquez, M. E. Vázquez, J. B. Blanco, L. Castedo, J. L. Mascareñas, *Angew. Chem.* **2007**, *119*, 7010–7014; *Angew. Chem. Int. Ed.* **2007**, *46*, 6886–6890; b) J. B. Blanco, V. I. Dodero, M. E. Vázquez, M. Mosquera, L. Castedo, J. L. Mascareñas, *Angew. Chem.* **2006**, *118*, 8390–8394; *Angew. Chem. Int. Ed.* **2006**, *45*, 8210–8214; c) J. B. Blanco, O. Vázquez, J. Martínez-Costas, L. Castedo, J. L. Mascareñas, *Chem. Eur. J.* **2005**, *11*, 4171–4178; d) J. B. Blanco, M. E. Vázquez, J. Martínez-Costas, L. Castedo, J. L. Mascareñas, *Chem. Biol.* **2003**, *10*, 713–722; e) M. E. Vázquez, A. M. Caamaño, J. Martínez-Costas, L. Castedo, J. L. Mascareñas, *Angew. Chem.* **2001**, *113*, 4859–4861; *Angew. Chem. Int. Ed.* **2001**, *40*, 4723–4725; f) J. B. Blanco, M. E. Vázquez, L. Castedo, J. L. Mascareñas, *ChemBioChem* **2005**, *6*, 2173–2177.

[7] a) N. G. Nickols, C. S. Jacobs, M. E. Farkas, P. B. Dervan, *Nucleic Acids Res.* **2007**, *35*, 363–370; b) B. S. Edelson, T. P. Best, B. Olenyuk, N. G. Nickols, R. M. Doss, S. Foister, A. Heckel, P. B. Dervan, *Nucleic Acids Res.* **2004**, *32*, 2802–2818; c) T. P. Best, B. S. Edelson, N. G. Nickols, P. B. Dervan, *Proc. Natl. Acad. Sci. USA* **2003**, *100*, 12063–12068; d) K. S. Crowley, D. P. Phillion, S. S. Woodard, B. A. Schweitzer, M. Singh, H. Shabany, B. Burnette, P. Hippenmeyer, M. Heitmeier, J. K. Bashkin, *Biorg. Med. Chem. Lett.* **2003**, *13*, 1565–1570.

[8] It is known that the presence of alkylamine side chains on DNA minor-groove binding fragments increases their DNA affinity: a) A. L. Kahane, T. C. Bruice, *Bioorg. Med. Chem. Lett.* **2006**, *16*, 6255–6261; b) A. L. Satz, T. C. Bruice, *Acc. Chem. Res.* **2002**, *35*, 86–95; charged peptides can bind unspecifically to DNA phosphates: c) A. Zlotnick, S. L. Brenner, *J. Mol. Biol.* **1989**, *209*, 447–457; d) K. A. Browne, G.-X. He, T. C. Bruice, *J. Am. Chem. Soc.* **1993**, *115*, 7072–7079.

[9] a) E. A. Goun, T. H. Pillow, L. R. Jones, J. B. Rothbard, P. A. Wender, *ChemBioChem* **2006**, *7*, 1497–1515; b) S. Futaki, *Adv. Drug Delivery Rev.* **2005**, *57*, 547–558; c) J. B. Rothbard, E. Kreider, C. L. Vandeusen, L. Wright, B. L.; Wylie, P. A. Wender, *J. Med. Chem.* **2002**, *45*, 3612–3618; Wylie, P. A. Wender, *J. Med. Chem.* **2002**, *45*, 3612–3618; d) L. R. Wright, J. B. Rothbard, P. A. Wender, *Curr. Protein Pept. Sci.* **2003**, *4*, 105–124.

[10] a) D. Rentzeperis, L. A. Marky, T. J. Dwyer, B. H. Geierstanger, J. G. Pelton, D. E. Wemmer, *Biochemistry* **1995**, *34*, 2937–2945; b) C. Bailly, J. Chaires, *Bioconjugate Chem.* **1998**, *9*, 513–538; c) M. Coll, C. A. Frederick, A. H.-J. Wang, A. Rich, *Proc. Natl. Acad. Sci. USA* **1987**, *84*, 8385–8389; d) K. Uyt-

terhoeven, J. Sponer, L. V. Meervelt, *Eur. J. Biochem.* **2002**, *269*, 2868–2877.
[11] a) R. Baliga, D. M. Crothers, *Proc. Natl. Acad. Sci. USA* **2000**, *97*, 7814–7818; b) R. Baliga, E. E. Baird, D. M. Herman, C. Melander, P. B. Dervan, D. M. Crothers, *Biochemistry* **2001**, *40*, 3–8.
[12] C. Costas, J. Martinez-Costas, G. Bodelón, J. Benavente, *J. Virol.* **2005**, *79*, 2141–2150.
[13] a) D. DiDonato, D. L. Brasaemle, *J. Histochem. Cytochem.* **2003**, *51*, 773–780; b) R. W. Hoetelmans, F. A. Prins, V. I. Corneleseten, J. van der Meer, C. J. van der Velde, J. H. van Dierendonck, *Appl. Immunohistochem.* **2001**, *9*, 346–351.
[14] For a related intracellular disulfide cleavage, see: C. N. Carrigan, B. Imperiali, *Anal. Biochem.* **2005**, *341*, 290–298.
[15] E. K. Liebler, U. Diederichsen, *Org. Lett.* **2004**, *6*, 2893–3896.
[16] W. S. Hancock, J. E. Battersby, *Anal. Biochem.* **1976**, *71*, 260–264.
[17] P. Lloyd-Williams, G. Jou, F. Albericio, E. Giralt, *Tetrahedron Lett.* **1991**, *32*, 4207–4210.
[18] a) I. Annis, L. Chen, G. Barany, *J. Am. Chem. Soc.* **1998**, *120*, 7226–7238; b) G. T. Hermanson, *Bioconjugate Techniques*, Academic Press, San Diego, **1996**, pp. 151–152 and 132–133.

Received: May 23, 2008
Published online on October 22, 2008

